REPORT DOCUMENTATION PAGE

1. REPORT DATE (DD-MM-YYYY) 4 Aug 2000	2. REPORT TYPE Journal Article	3. DATES COVERED (From - To) 5/98 – 5/00

4. TITLE AND SUBTITLE A new energy transfer chemical laser at 1.315 microns	5a. CONTRACT NUMBER
	5b. GRANT NUMBER
	5c. PROGRAM ELEMENT NUMBER
6. AUTHOR(S) Thomas L. Henshaw, Gerald C. Manke II, Timothy J. Madden, Michael R. Berman, Gordon D. Hager	5d. PROJECT NUMBER 3326
	5e. TASK NUMBER LA
	5f. WORK UNIT NUMBER 02

7. PERFORMING ORGANIZATION NAME(S) AND ADDRESS(ES) Air Force Research Laboratory Directed Energy Directorate 3550 Aberdeen Ave. SE Kirtland AFB, NM 87117	8. PERFORMING ORGANIZATION REPORT NUMBER

9. SPONSORING / MONITORING AGENCY NAME(S) AND ADDRESS(ES) Air Force Research Laboratory Directed Energy Directorate 3550 Aberdeen Ave. SE Kirtland AFB, NM 87117	10. SPONSOR/MONITOR'S ACRONYM(S)
	11. SPONSOR/MONITOR'S REPORT NUMBER(S)

12. DISTRIBUTION / AVAILABILITY STATEMENT
Approved for public release; distribution is unlimited

14. ABSTRACT
CW laser action has been demonstrated on the electronic I* - I transition of atomic iodine at 1.315 microns from the NCL(a) + I energy transfer reaction. The stimulated emission was generated in a transverse subsonic flow device when hydrogen azide, HN3, was injected into a flow of iodine and chlorine atoms. The measured laser output power was 180mW.

20020905 068

15. SUBJECT TERMS
chemical lasers, chemical iodine lasers, AGIL, energy transfer, COIL

16. SECURITY CLASSIFICATION OF:			17. LIMITATION OF ABSTRACT	18. NUMBER OF PAGES	19a. NAME OF RESPONSIBLE PERSON Gerald C. Manke II
a. REPORT Unclassified	b. ABSTRACT Unclassified	c. THIS PAGE Unclassified	Unlimited	9	19b. TELEPHONE NUMBER (include area code) 505-853-2674

A new energy transfer chemical laser at 1.315 μm

Thomas L. Henshaw *, Gerald C. Manke II, Timothy J. Madden,
Michael R. Berman [1], Gordon D. Hager

*Gas and Chemical Lasers Branch, Directed Energy Directorate, Air Force Research Laboratory / DELC, 3550 Aberdeen Ave. SE,
Kirtland AFB, NM 87117-5776, USA*

Abstract

CW laser action has been demonstrated on the electronic $I^*(^2P_{1/2}) \rightarrow I(^2P_{3/2})$ transition of atomic iodine at 1.315 μm from the NCl $(a^1\Delta) + I(^2P_{3/2})$ energy transfer reaction. The stimulated emission was generated in a transverse subsonic flow device when hydrogen azide, HN_3, was injected into a flow of iodine and chlorine atoms. The measured laser output power was 180 mW. © 2000 Elsevier Science B.V. All rights reserved.

1. Introduction

Chemical lasers are devices that derive their population inversions from exothermic chemical reactions, whether directly or indirectly, and include photochemical-induced bond dissociation, radiative recombination of atoms or molecules and energy transfer (ET) processes. In view of their generally efficient conversion of chemical potential into laser radiation, chemical lasers have been sought after for numerous applications in which lightweight, self-contained lasers are utilized. The advent of chemical lasers began with experiments conducted by Kasper and Pimentel in 1965, who successfully demonstrated lasing on various vibrational levels of HCl obtained by photolysis of H_2/Cl_2 mixtures [1]. A short time thereafter, Cool et al. demonstrated the

first purely chemical laser using fluorine atom combustion technology to initiate lasing in the DF/CO_2 system [2]. It was not until 1978 that McDermott and co-workers demonstrated the first chemically pumped electronic transition laser [3,4]. Continuous wave (cw) laser oscillation was achieved on the $I^*(^2P_{1/2})-I(^2P_{3/2})$ transition via the ET reaction between the oxygen metastable, $O_2 (a^1\Delta)$, and a ground state iodine atom, $I(^2P_{3/2})$. This chemistry forms the basis of the high-powered Chemical Oxygen Iodine Laser, or COIL, which operates in the near-infrared at 1.315 μm with cw power up to 40 kW.

Long lived metastables are noted for their importance as energy carriers in chemical laser media and identifying suitable electronically excited metastables for short wavelength laser utility has been the focus of extensive work over several decades [5–9]. Of considerable interest are the nitrene metastables NCl $(a^1\Delta)$ and NF $(a^1\Delta)$, which are isovalent with $O_2 (a^1\Delta)$ and possess many favorable properties as energy carriers in a chemically pumped laser system.

---
* Corresponding author. Fax: +1-505-846-4807; e-mail: thomas.henshaw@kirtland.af.mil
[1] Air Force Office of Scientific Research/NL, 801 North Randolph Street, Room 732, Arlington, VA 22203-1977, USA.

Among these are long radiative lifetimes [10,11] and efficient gas phase chemical generation [10–13]. In fact, following the discovery of the efficient electronic ET between NCl (a$^1\Delta$) and atomic iodine [14,15],

$$NCl(a^1\Delta) + I(^2P_{3/2}) \rightarrow NCl(X^3\Sigma) + I^*(^2P_{1/2}) \quad (1)$$

$$I^*(^2P_{1/2}) \rightarrow I(^2P_{3/2}) + h\nu(1.315\,\mu m), \quad (2)$$
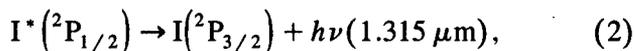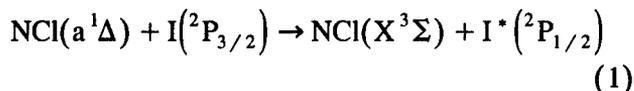
several laboratories have attempted the demonstration of gain and or lasing on the 1.315 μm transition of atomic iodine using this mechanism. In 1992, Yang et al. provided evidence of an I*($^2P_{1/2}$)–I($^2P_{3/2}$) population inversion in a subsonic flow using chemically generated NCl (a$^1\Delta$) [16] and shortly thereafter near threshold laser oscillation was observed in the NCl (a$^1\Delta$)–I*($^2P_{1/2}$) system by Ray and Coombe from the pulsed ArF laser photolysis of ClN$_3$ and CH$_2$I$_2$ [17]. Recently, this laboratory reported for the first time a direct and quantitative measurement of the population inversion between the ($^2P_{3/2}$) and ($^2P_{1/2}$) states of atomic iodine produced by energy transfer from NCl (a$^1\Delta$) [18]. This effort represented a significant milestone in the development of a chemically pumped, all gas phase iodine laser. In continuing our investigation into the NCl (a$^1\Delta$)/I*($^2P_{1/2}$) ET system, we report for the first time an example of continuous wave I*($^2P_{1/2}$)–I($^2P_{3/2}$) laser oscillation resulting from entirely gas phase chemical generation.

2. Experimental

The demonstration of I*($^2P_{1/2}$)–I($^2P_{3/2}$) laser action was performed in a transverse subsonic flow reactor shown in Fig. 1. The essential features of this apparatus are a dc discharge for F atom production, an axial injector for DCl injection, and two side-wall transverse injectors for HI and HN$_3$ admission into the flow stream. In addition, the apparatus is equipped with sensitive optical diagnostics for measuring optical gain between the I($^2P_{3/2}$)–I*($^2P_{1/2}$) states. Experimental details of the gain measurement and methodology have been described

elsewhere [19–21] and only a brief discussion is presented here.

The laser cavity consisted of 5 cm wide times 2 cm high stainless steel duct (cross-sectional area = 10 cm^2) whose inner surfaces were lined with Teflon ramps and flow shrouds to minimize wall deactivation and help confine the active gain zone to a nominal 5 cm length. The resonator mirrors (M1 and M2 in Fig. 1) were 2.54 cm in diameter and were mounted on two 2.54 cm (OD) vacuum tubes with mirror bellows and micrometers for alignment. The mirrors were separated by 1.15 m and purged with He during laser operation. The reactor wall height (2 cm) and the inside diameter of the mirror mount (2 cm) adjoining the mirrors to the vacuum tubes defined the minimum aperture of the cavity. Laser power measurements were conducted under a variety of optical resonator conditions. However, owing to the potentially small signal gain of the system, the initial resonator was fitted with two symmetric 5 m concave ultra-high finesse cavity mirrors (Research Electro Optics Corp). These mirrors were primarily used to overcome cavity losses and confirm the presence of stimulated emission. The high finesse mirrors were characterized by cavity-ring-down spectroscopy (Los Gatos Research, Los Gatos, CA) which revealed a high reflectivity of 99.998 ± 0.001% at 1.32 μm; however, measurement of transmission and substrate absorption/scattering losses were not performed. Subsequent to the initial laser demonstration, additional power extraction experiments were conducted using various output couplers listed at a nominal 99.9% reflectivity (CVI, Inc.) and the high finesse back reflector of 99.998% reflectivity. Coarse alignment was obtained by first superimposing a He:Ne laser beam through the centerline of the flow reactor and then adjusting the resonator mirrors such that reflected beams from the resonator mirrors are collinear with the reactor centerline. The laser power output was measured with an Ophir power meter (Model PD 300-IR Nova) for tests in the 0–30 mW range and a Coherent meter (Model 210) for powers above 30 mW.

The observation of small signal gain on the I($^2P_{3/2}$)–I*($^2P_{1/2}$) transition was measured with a continuously tunable, single-mode 1.315 μm diode laser with a spectral line width of less than 500 kHz (FWHM) over 30 GHz from 7602.4 to 7603.5 cm^{-1}.
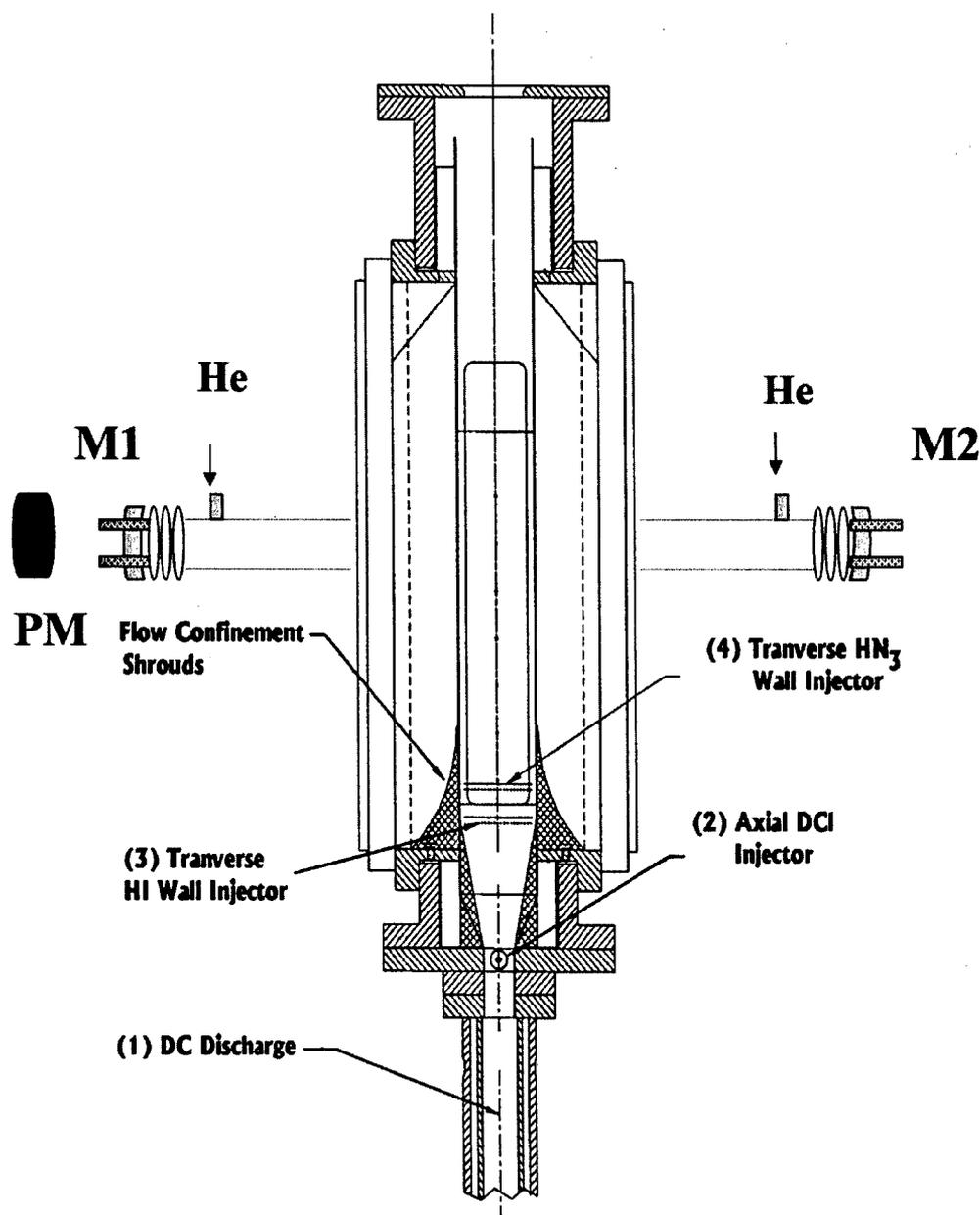
Fig. 1. Schematic representation of the subsonic flow device and optical resonator showing (1) dc discharge, (2) axial injector (DCl), (3) first set of transverse wall injectors (HI), (4) second set of transverse wall injectors (HN$_3$) and (5) flow confinement shrouds. The optical cavity, consisting of mirrors M1 and M2, is joined to the flow tube by two tubes containing mirror mounts, bellows and micrometers for alignment. Each tube is purged with He and the out-coupled laser power measured with a power meter (PM).

This performance allows the laser to scan across the entire $I(^2P_{3/2})$–$I^*(^2P_{1/2})$ transition with complete hyperfine resolution. Since the F(3,4) transition in iodine exhibits the highest gain among the hyperfine lines, it was used to monitor the $I(^2P_{3/2}) \rightarrow I^*(^2P_{1/2})$ gain. The diode laser is operated in a double-pass arrangement providing a pathlength of 10 cm.

Fluorine atoms are generated using a 10 kW dc discharge (1.75 kW actual power load when running) of F$_2$ or NF$_3$ in helium. The pressure in the system was regulated by flowing N$_2$ 1.5 m downstream of

the reactor cavity through a 3 cm choke orifice. Flow reactor pressures were measured with calibrated absolute capacitance manometers. Reagents introduced into the flow stream were measured with either calibrated mass flow controllers or sonic orifices. Hydrogen azide was synthesized by the reaction of molten stearic acid $(CH_3(CH_2)_{16}COOH)$ with sodium azide (NaN_3), under vacuum at $110°C$. A $10:1$ molar excess of stearic acid over sodium azide was used. The gaseous HN_3 was stored as a 10% mixture in helium. Helium diluent (Matheson, 99.995%), F_2 (Matheson, 20% in He), NF_3 (Spectra Gas, 99%), DCl (Cambridge Isotopes, 99%), HI (Matheson, 99%) were used without further purification.

The chemical generation of $I^*(^2P_{1/2})$ and subsequent lasing is based on a sequential process in which Cl and I atoms are produced,

$$F + DCl \rightarrow DF + Cl, \quad k_{300\,K} = 1 \times 10^{-11}\,cm^3/s;$$

see Ref. [22]; (3)

$$Cl + HI \rightarrow HCl + I(^2P_{3/2}),$$

$$k_{300K} = 1.0 \times 10^{-10}\,cm^3/s; \quad \text{see Ref. [23]}; \quad (4)$$
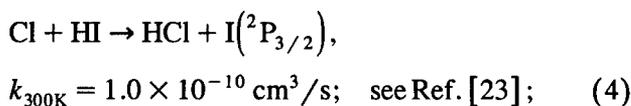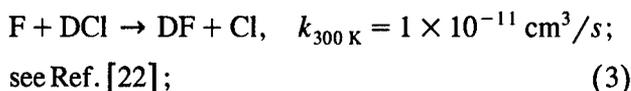
followed by $NCl\,(a^1\Delta)$ production,

$$Cl + HN_3 \rightarrow HCl(v) + N_3, k_{300K}$$
$$= 1 \times 10^{-12}\,cm^3/s; \quad \text{see Ref. [24]}; \quad (5)$$

$$Cl + N_3 \rightarrow NCl(a^1\Delta, b^1\Sigma, X^3\Sigma) + N_2(X^1\Sigma), k_{300K}$$
$$= 2 \times 10^{-11}\,cm^3/s; \quad \text{see Refs. [12,13]}; \quad (6)$$
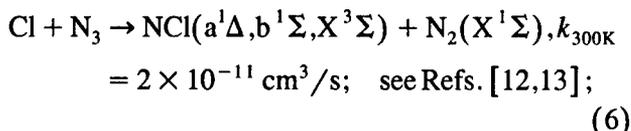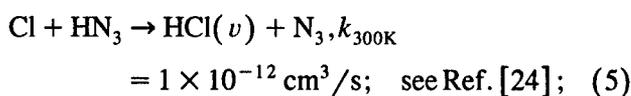
and finally the ET reaction between $NCl\,(a^1\Delta)$ and $I(^2P_{3/2})$ to generate $I^*(^2P_{1/2})$: [12,15]

$$NCl(a^1\Delta) + I(^2P_{3/2}) \rightarrow NCl(X^3\Sigma) + I^*(^2P_{1/2}),$$

$$k_{300K} = 2 \times 10^{-11}\,cm^3/s \quad (7)$$

$$I^*(^2P_{1/2}) + h\nu \rightarrow I(^2P_{3/2}) + nh\nu\,(1.315\,\mu m).$$
$$(8)$$
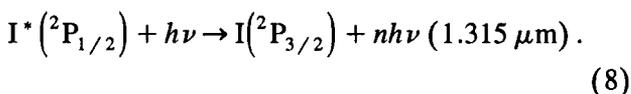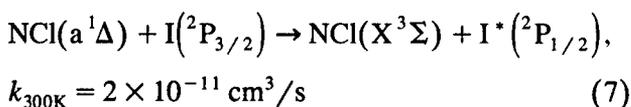
The magnitude of these room temperature rate coefficients indicate a rapid mechanism for the generation of $NCl\,(a^1\Delta)$ and $I^*(^2P_{1/2})$, notwithstanding the small room temperature $Cl + HN_3$ rate coefficient in reaction (5). Indeed, its value suggests it is rate limiting and that minimal N_3 formation, and

hence, $NCl\,(a^1\Delta)$ density would be generated via this reaction. However, a recent temperature-dependent study on the $Cl + HN_3$ reaction rate coefficient over the 300–500 K range reveals a significant temperature dependence with $k(T) = 1.2 \pm 0.3 \times 10^{-11}T^{1/2}\,exp(-1514 \pm 93/T)$ [24]. Using the 1.315 μm diode laser, an analysis of the I-atom line shape shows a Doppler broadened linewidth that corresponds to an apparent temperature upwards of 650 K. In this regard, a strong enhancement in this reaction rate is expected and a sizable portion of N_3 density is subsequently generated through this reaction chemistry. Furthermore, since both the branching fractions for $NCl\,(a^1\Delta)$ and $I^*(^2P_{1/2})$ in reactions (6) and (7) are reported to exceed 50%, the mechanism described here depicts an efficient gas phase chemical process for the production of $NCl\,(a^1\Delta)$ and $I^*(^2P_{1/2})$ [12,13,15].

Experimentally, the $I^*(^2P_{1/2})$ inversion density is obtained by an ordered injection of DCl, followed by HI and finally HN_3 into the flow reactor. The staging of this injection sequence is important for the following considerations. First, a condition of excess F atoms must be avoided to eliminate the competing reactions:

$$F + HN_3 \rightarrow HF(v) + N_3,$$

$$k_{300K} = 1.1 \times 10^{-10}\,cm^3/s; \quad (9)$$

$$F + N_3 \rightarrow NF(a^1\Delta) + N_2,$$

$$k_{300K} = 5 \times 10^{-11}\,cm^3/s; \quad (10)$$

$$F + NCl(a) \rightarrow products,$$

$$k_{300K} = 2 \times 10^{-11}\,cm^3/s; \quad \text{see Ref. [13]}, \quad (11)$$
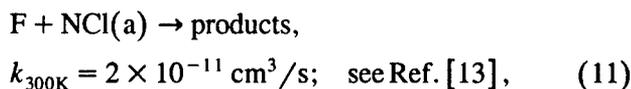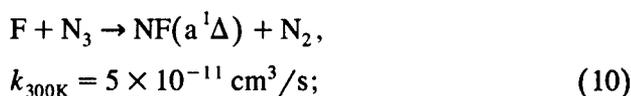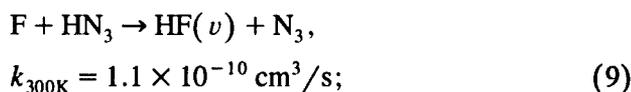
which ultimately deplete the system of $NCl\,(a^1\Delta)$ production and hence, $I^*(^2P_{1/2})$. Thus, the DCl flow is typically run in two-fold excess over the measured F atom flow rate. Further, utilizing DCl as a Cl atom source is necessary to eliminate the production of HF, which is an effective quencher of $I^*(^2P_{1/2})$ [25]. Once the F atoms are converted into Cl, the reactions of Cl with HI and HN_3 proceed with production of ground state I, $NCl(a^1\Delta)$ and HCl, which is a relatively benign quencher of $NCl(a^1\Delta)$ and $I^*(^2P_{1/2})$. The injection of HI precedes HN_3 in order to have $I(^2P_{3/2})$ atoms present in the flow stream when $NCl\,(a^1\Delta)$ is produced. This minimizes the bimolecular $NCl\,(a^1\Delta)$ self-annihilation rate,

$k = 7 \times 10^{-12}$ cm^3/s, a deleterious effect that would be considerable at the densities present in these experiments [26].

3. Results and discussion

Although F$_2$ has been successfully used to generate gain in this system, the best peak gains were obtained when NF$_3$ was used as an F atom source. As such, Fig. 2 presents a summary of gain scaling with respect to various HN$_3$ flows ranging from 2.0 to 5.3 mmol/s for fixed flows of NF$_3$ at 2.4 mmol/s, DCl at 2.0 mmol/s and HI at 0.07 mmol/s and a total pressure of 16 Torr. The data was collected 7 cm downstream from the HN$_3$ injection point, which is the stream-wise position of maximum gain for the I*(^{2}P$_{1/2}$)–I(^{2}P$_{3/2}$) transition. It is not clear as to what the operative mechanism is that facilitates the improved gain with NF$_3$. However, in a previous study it was determined that conversion of F$_2$ to F atoms in the discharge is incomplete and significant amounts of F$_2$ flow into the reactor cavity [27,28]. This may result in IF production through the secondary F$_2$ + I → IF reaction which promotes efficient I*(^{2}P$_{1/2}$) quenching.
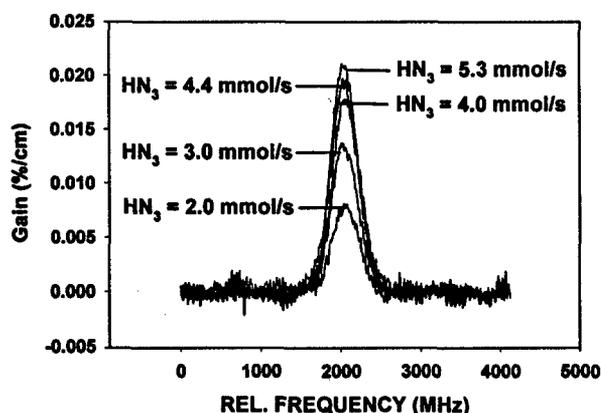

Fig. 2. A summary of gain scaling with respect to various HN$_3$ flows ranging from 2.0 to 5.3 mmol/s for fixed flows of NF$_3$ = 2.4 mmol/s, DCl = 2.0 mmol/s, HI = 0.07 mmol/s, and a total pressure of 16 Torr. The He bath gas constitutes 95% of the total gas flow. The data was collected 7 cm downstream from the HN$_3$ injection point, which is the stream-wise position of maximum gain for the I*(^{2}P$_{1/2}$)–I(^{2}P$_{3/2}$) transition. Under these conditions, the maximum small signal gain, $g_0 = 2.1 \times 10^{-4}$ cm^{-1}, was obtained at an HN$_3$ flow of 5.3 mmol/s.

The gain measured in Fig. 2 represents the necessary but not sufficient condition for laser oscillation. The conditions under which laser action will occur depends on the mirror reflectances; strictly speaking this is when the gain exceeds or is at least equal to the losses in the resonator. Thus, the immediate goal is to identify what cavity parameters, specifically mirror reflectance values, over which power can be extracted. Considering only the optical losses occurring at the mirror ports, the useful power (that is, the power transmitted to the power meter) is constrained by mirror reflectivity (R), transmittance (T), scattering (S) and absorbance (A). Since the scattering-absorption losses and, to a lesser degree, transmission of available laboratory mirrors have not been quantified, a rigorous maximization of output power via mirror reflectivity was not performed. Nevertheless, the outcoupling power of the laser exhibits certain characteristic features; namely there exists a range of mirror reflectivities over which power can be extracted and an optimum reflectivity that determines maximum output power. In this regard, the gain measurements obtained here are used to determine the required range of mirror reflectivities where laser power can be extracted but not necessarily the optimum power.

The gain, g, in the active medium when lasing is present in this analysis is given by

$$g = \frac{7}{12} \frac{\lambda^2 A_{3,4}}{8\pi} f(\nu_0) \left(\left[I^*\left(^2P_{1/2}\right) \right] - \frac{1}{2} \left[I\left(^2P_{3/2}\right) \right] \right)$$

$$= \sigma_{3,4} \Delta N \tag{12}$$

where λ is the wavelength (1.315 μm), $A_{3,4}$ is the Einstein coefficient (5.08 s^{-1}) and $f(\nu)$ is the normalized line shape function for spectral broadening. In the absence of stimulated emission, the population density of I*(^{2}P$_{1/2}$) and I(^{2}P$_{3/2}$) are not perturbed and Eq. (12) is distinguished by $g_0 = \sigma_{3,4}$ ([I*(^{2}P$_{1/2}$)]$_0$–1/2[I(^{2}P$_{3/2}$)]$_0$), which is the small signal gain. Under steady state conditions, where the only losses are assumed to be occurring at the mirror output ports, the saturated gain, g, is

$$g = \frac{-\ln R_1 R_2}{2L} \tag{13}$$

where R_1 and R_2 are mirror reflectivities and L is the cavity path length. This relates the minimum gain

to the design features of the oscillator. When $R = R_{min}$, the minimum reflectance at threshold, the I and I^* inversion density is unperturbed and $g = g_0$ and the laser just begins to oscillate. As the reflectivity is increased the cavity losses are overcome and the output power increases concurrently until a maximum is reached. In the limit as the cavity losses go to zero, the optimum reflectivity approaches unity and the maximum power occurs at zero output coupling. However, when $R \rightarrow 1$ small but finite losses such as a distributed non-saturable loss, diffraction, scattering and mirror absorption can become comparable to the transmitted power in which case the power falls off.

The mirror reflectivity, R_1, that is required to overcome losses due to threshold laser action is

$$R_1 = \frac{e^{-2Lg_0}}{R_2}. \tag{14}$$

Accordingly, using the maximum $g_0 = 2.1 \times 10^{-4}$ cm^{-1} obtained from Fig. 2, $L = 5$ cm and letting $R_2 = 0.99998$, the minimum reflectivity R_1 required to overcome cavity losses is 0.9979. Similarly, allowing $R_1 = R_2 = 0.99998$, the minimum gain at threshold is 4×10^{-6} cm^{-1}. Consequently, the values of R_1 (taken as R_{min}) and R_2 (0.99998) bound the extractable power to range of mirror transmissions, $T = 1 - R$, between 2×10^{-5} and 2.1×10^{-3}. Since this is a very narrow transmission region, a resonator was specifically designed with two ultra-high finesse mirrors in order to confidently overcome cavity losses and ensure laser action, but not necessarily achieve maximum laser power. Thus, once lasing was demonstrated output couplers of lower nominal reflectivity, within the range 0.99998

$> R > 0.9979$, were examined for their effect on extracting higher laser power.

The high finesse optical cavity consisted of two symmetric mirrors (M1 and M2 in Fig. 1) with 0.99998 reflectivity at 1.32 μm and 5 m radius of curvature. The flow reactor and resonator conditions for demonstrating lasing are tabulated in Trial 1, Table 1. Evidence of laser action was demonstrated by measuring the output power on a calibrated power meter. Thus, upon adding HN_3 to a steady stream of Cl and I atoms, 3 mW of power was measured per mirror port for a total of 6 mW. In addition, the mode pattern of the laser was easily observed on a near-IR phospor card (1.3 μm) at a distance of 2 m from the output coupler (M1). In contrast, upon misaligning the cavity or turning off any of the fuels, the laser power signal was immediately extinguished and returned to baseline. The laser run time is typically 20–30 s; however, this period of operation simply was performed only to conserve the HN_3 fuel. Longer run times of up to several minutes are possible and are only limited by the storage volume and pressure of our HN_3 reservoir (300 L).

In keeping with the measured g_0 and reflectance range defined above, attempts at extracting more power from the cavity were performed by replacing the output coupler (M1) with a more transmissive mirror. In this vein, two mirrors with vendor quoted nominal reflectance values of 0.998 R (2 m cc) and 0.999 R (2 m cc) were tested for output power. In an effort to characterize these mirrors more fully, several independent in-house transmission measurements were performed on these mirrors using the 1.315 μm gain probe laser. However, no attempt at specifying the mirror scattering or absorption was performed. For purposes of clarity, the 0.998 R and

Table 1

Flow reactor and resonator conditions for achieving laser action on the $I^*(^2P_{1/2})-I(^2P_{3/2})$ transition

Trial	Flow reactor conditions							Resonator conditions		
	He (mmol/s)	NF$_3$ (mmol/s)	DCL (mmol/s)	HN$_3$ (mmol/s)	HI (mmol/s)	P (Torr)	Zone (cm)	HR	OC	Power (mW)
1	128.80	1.08	2.11	3.16	0.04	15.73	15	0.99998	0.99998	6
2	127.86	1.02	2.20	3.03	0.04	15.61	15	0.99998	0.9988 (I)	19
3	149.78	1.53	2.22	4.36	0.07	14.67	15	0.99998	0.9988 (I)	110
4	141.73	1.51	2.40	4.59	0.07	14.95	15	0.99998	0.9988 (II)	180

0.999 R mirrors were labeled OC I and OC II, respectively. Accordingly, results from these measurements give an average transmisson of $1.2 \pm 0.1 \times 10^{-3}$ ($R = 0.9988 \pm 0.0001$) for both OC I and OC II and thus, within experimental uncertainty, there is no apparent difference in the reflectance values between these two mirrors. Trial 2 in Table 1 shows the effect of substituting the high finesse outcoupler with OC I, $R = 0.9988$. For near identical flow conditions, the output power more than triples. Indeed, using OC I under the enhaced NF_3, HN_3 and HI flow conditions shown in Trial 3 the power increases considerably to 110 mW. Interestingly, in Trial 4 the power extraction is repeated with OC II, $R = 0.9988$, and a significant power enhancement to 180 mW is observed. Since the transmission measurements for OC I and II are somewhat limited in accuracy, the power enhancement shown with OC II may be attributed to slight variations in the magnitude of the mirror transmission that are not discernable by these measurements, or possibly by other systematic effects such as better cavity alignment. It should be noted that although attempts were made at keeping the flow rates constant, the recorded HN_3 and DCl flow rates in Trial 4 were slightly higher and thus may also have contributed to the overall increase in power.

4. Summary and conclusion

A new, chemically pumped, continuous wave laser operating on the $I(^2P_{3/2})–I^*(^2P_{1/2})$ transition of iodine at 1.315 μm has been demonstrated. The laser is based on the ET reaction between metastable NCl $(a\,^1\Delta)$ and ground state $I(^2P_{3/2})$ atoms. This represents a significant step in the development of a chemically pumped, all gas phase iodine laser. The efficiency of the laser at this time is not fully characterized since the current device features small gain, pathlength and limitations in the amount of fluorine atoms that can be generated in this device. Future work will be directed at constructing a larger device with longer pathlength and higher mass flow rates to enhance the single-pass gain and mode volume of this system. In addition, continued efforts will be directed at obtaining a more detailed understanding of the mixing and chemical kinetics of this system

and the subsequent role they play on laser performance.

References

[1] J.V.V. Kasper, G.C. Pimentel, Appl. Phys. Lett. 5 (1964) 231.
[2] T.A. Cool, R.R. Stevens, T.J. Falk, Int. J. Chem. Kinet. 1 (1970) 295.
[3] W.E. McDermott, N.R. Pchelkin, D.J. Benard, R.R. Bousek, Appl. Phys. Lett. 32 (1978) 469.
[4] D.J. Benard, W.E. McDermott, N.R. Pchelkin, R.R. Bousek, Appl. Phys. Lett. 34 (1979) 40.
[5] J.M. Herbelin, N. Cohen, Chem. Phys. Lett. 20 (1973) 605.
[6] T.C. Clark, M.A.A. Clyne, Trans. Faraday Soc. 66 (1970) 877.
[7] C.T. Cheah, M.A.A. Clyne, J. Chem. Soc. Faraday Trans. 2/76 (1980) 1543.
[8] A.T. Pritt Jr., R.D. Coombe, Int. J. Chem. Kinet. 12 (1980) 741.
[9] M.A.A. Clyne, A.J. MacRobert, J. Brunning, C.T. Cheah, J. Chem. Soc. Faraday Trans. 2/79 (1983) 1515.
[10] J. Habdas, S. Watengaonkar, D.W. Setser, J. Phys. Chem. 91 (1987) 451.
[11] D.R. Yarkony, J. Chem. Phys. 86 (1987) 1642.
[12] R.J. Malins, D.W. Setser, J. Phys. Chem. 95 (1981) 1342.
[13] T.L. Henshaw, S.D. Herrera, L.A. Schlie, J. Phys. Chem. A 102 (1998) 6239.
[14] G.C. Manke II, D.W. Setser, J. Phys. Chem. A 102 (1998) 7257.
[15] R.D. Bower, T.T. Yang, J. Opt. Soc. Am. B 8 (1991) 1583.
[16] A.J. Ray, R.D. Coombe, J. Phys. Chem. 97 (1993) 3475.
[17] T. Yang, V.T. Gylys, R.D. Bower, L.F. Rubin, Opts. Lett. 24 (1992) 1803.
[18] A.J. Ray, R.D. Coombe, J. Phys. Chem. 99 (1995) 7849.
[19] J.M. Herbelin, T.L. Henshaw, B.D. Rafferty, B.T. Anderson, R.F. Tate, T.J. Madden, G.C. Manke II, G.D. Hager, Chem. Phys. Lett. 299 (1999) 583.
[20] R.F. Tate, B.T. Anderson, P.B. Keating, G.D. Hager, Proc. SPIE Gas Chem. Lasers Intense Beam Appl. 3268 (1998) 115.
[21] B.D. Rafferty, B.T. Anderson, T.L. Henshaw, J.M. Herbelin, G.D. Hager, Lasers 97 (1997) 23.
[22] T.L. Henshaw, T.J. Madden, J.M. Herbelin, G.C. Manke II, B.T. Anderson, R.F. Tate, G.D. Hager, Paper 3612-24, SPIE

Conference on Gas and Chemical Lasers and Intense Beam Applications II, San Jose, CA, January 1999.

[23] M.A.A. Clyne, W.S. Nip, Int. J. Chem. Kinet. 10 (1978) 367.

[24] F.J. Wodarczyk, C.B. More, Chem. Phys. Lett. 26 (1974) 484.

[25] G.C. Manke II, T.L. Henshaw, T.J. Madden, G.D. Hager, Chem. Phys. Lett. 310 (1999) 111.

[26] R.D. Coombe, A.T. Pritt Jr., J. Chem. Phys. 66 (1977) 5214.

[27] T.L. Henshaw, S.D. Herrera, L.A. Schlie, J. Phys. Chem. A 101 (1997) 4048.

[28] G.C. Manke II, T.L. Henshaw, T.J. Madden, J.M. Herbelin, B.D. Rafferty, G.D. Hager, accepted for publication in J. AIAA, April 2000.